An efficient approximation for the vibro-acoustic response of a turbulent boundary layer excited panel

Daniel Mazzoni

An efficient approximation for the vibro-acoustic response of a turbulent boundary layer excited panel

D. Mazzoni
Laboratoire de Mécanique et d'Acoustique
Ecole Supérieure de Mécanique de Marseille
IMT, Technopôle de Château-Gombert
13451 MARSEILLE CEDEX 20 (France)

Number of pages = 43

Number of figures = 9

MAZZONI Daniel
ESM2
IMT, Technopôle de Château-Gombert
13451 MARSEILLE CEDEX 20 (France)

Abstract

The aim of this study was to present a deterministic model for approximating the vibrations and the acoustic pressure radiated when a thin elastic plate is immersed in a low Mach number flow of fluid. As a prelude to this study, a classical random model based on a wavevector integration technique was used. In the case of a low Mach number turbulent flow, the numerical study showed that the subconvective region of the turbulent excitation power spectrum contributes importantly to the response of the panel. A deterministic approximate model was developed, based on this behaviour of the system.

1 Introduction

In the free space $I\!R^3$ consider the Cartesian set of coordinates $(0, \mathbf{x}, \mathbf{y}, \mathbf{z})$. A plane elastic rectangular panel Σ with length a, width b, and of constant thickness h is inserted into a flat infinite plane baffle. The panel Σ occupies the domain $[0, a] \times [0, b]$ of the $z = 0$ plane. For the sake of simplicity, it is assumed that the plate Σ is homogeneous and isotropic and that its motion can be modeled using the Kirchhoff-Helmholtz thin plate theory. The mechanical properties of this panel are a Young's modulus E, a Poisson coefficient ν and a mass per unit surface m. Let us take $\partial\sigma$ to denote the boundary of the panel Σ. The plate/baffle system separates two domains, the domain $z > 0$, denoted Ω, contains a perfect fluid characterized by a mass density ρ and a sound wave speed c. The fluid in the domain Ω is moving with the constant speed V in the direction parallel to the x-axis. A turbulent boundary layer develops at the interface between the fluid and the plate/baffle system. The wall pressure fluctuations in this turbulent boundary layer generate vibration in the plate and an acoustic radiation in the fluid. As regards the interactions between the structure and the turbulent flow, the model proposed here is based on the hypothesis that one-way interactions occur: Since the influence of the panel vibration on the boundary layer is neglected, the *blocked pressure* induced by the turbulent boundary layer is used as the forcing function. It is also assumed that when reaching the plate, the turbulent boundary layer is fully developed, and that the acoustic wave propagation is not affected by the flowing fluid. In order to simplify the expressions, the domain $z < 0$ is taken to be a vacuum, but it is also possible to study a fluid at rest in $z < 0$.

One of the first models for the vibro-acoustic response of a plane rectangular panel excited by a turbulent boundary layer was developed by Davies [1]. The latter author proposed a space integration method to define the power density functions of the displacement of the plate and of the radiated acoustic pressure. As the fluid in [1] was a gas, the author proposed an usual modal method with some developments to take advantage of the weak influence of the fluid on the vibration of the structure. In [2], a wavenumber integration technique was developed to investigate the spatial filtering characteristics of a rectangular menbrane. This technique was used to measure the low wavenumber components of the turbulence, corresponding to a region where the Corcos space-time correlation model did not give very good results. The authors of [3] analysed the coupling between the structural modes and the wavenumbers of a turbulent flow and proposed a wavenumber sensitivity function for a rectangular plate with various boundary conditions. This study showed how sensitive a plane panel is to the low wavenumber region of the turbulent boundary layer power spectrum. The flow induced noise inside an aircraft cabin was investigated by Graham in [4] and [5]. In [4], the sound radiation from a flat elastic plate under boundary layer excitation was determinated by performing a standard modal analysis and using a wavenumber integration technique. An estimate of the cabin noise was obtained by summing together the incoming power contributions of all the fuselage panels. In [5], this model was extended to take the wall acoustic treatment of the cabin into account. In [4] and [5] it was clearly established that the coupling between the acoustic field and the elastic structure is crucially dependent on the modal acoustic impedances. At higher Mach numbers, the author of [6] determined the influence of the mean flow on the acoustic radiation of the plate, and showed that the mean flow significantly reduces the frequency at which a resonant mode become an efficient radiator. In [7], the suitability of a model based on a wavenumber integration technique for predicting the vibro-acoustic response of an elastic plate coupled on one side with a fluid cavity and on the other side with a semi-infinite fluid domain and excited by a turbulent boundary layer was investigated in the case of a simple two-dimensional example. In [7], the autors showed the importance of the effects of the low wavenumber region of the turbulent boundary layer power spectrum on response of the structure. Since the model presented in [7] was two-dimensional, the influence of the transverse wavenumbers was neglected. A complete framwork of this wavenumber integration method is given in [8], where it is compared with the usual space interation method. To deal with cases where the fluid surrounding the plate is a gas, the authors of [8] expanded the vibro-acoustic responses of the panel into series of *fluid-loaded* eigenmodes and performed a *light-fluid* approximation to take advantage of the weak influence of the fluid on the vibration of the system. This *light-fluid* approximation consists in expanding the eigenmodes and eigenvalues of the plate/fluid system into series of a small parameter. Further details about this singular perturbation technique are given in [9]. An experimental validation of the method using both a space integration technique and a modal approach is proposed in [10] and [11]. The results predicted using a wavenumber integration method are compared with experimental data in [12].

In the present paper, the model presented in [7] is extented to a three-dimensional geometry, and approximations are proposed for both the power spectrum of the displacement of the plate and the power spectrum of the acoustic radiation, based on an analytical wavenumber integration procedure. This analytical integration procedure yields the definition of a turbulent force F_{TBL}, which can be used as a forcing function in a numerical model giving the vibro-acoustic responses of a panel excited by a deterministic force. The aim of this paper is to show that the results obtained with a deterministic model calculated from the forcing function F_{TBL} match the vibro-acoustic responses of a plate excited by a turbulent boundary layer. One advantage of using the deterministic force described here is the CPU savings involved, due to the fact that the wavenumber integrals are calculated in an analytical way. The second, and possible most important advantage, is that as the model defines a deterministic force F_{TBL} as being equivalent to a random excitation, it becomes easy to calculate the vibro-acoustic response of a panel excited by both a random and a deterministic force, since this amounts to simply merging two deterministic forces. As an example, this model should be most helpful when calculating the response of a panel subjected to both a turbulent flow of fluid and an acoustic noise.

This paper begins with the definition of a wavevector integration model for the vibro-acoustic response of the fluid-loaded structure. The influence of the low wavenumber region of the wavevector-frequency power spectrum of the turbulent excitation on the vibro-acoustic response of the system is investigated in section 5 by defining two functions, a wavevector transfer function and a wavevector density function. A deterministic approximate model is proposed in section 6 under the assumption that the response of the structure depends mainly on the low wavenumber region, or subconvective domain, of the turbulent boundary layer power spectrum. The predictions of this deterministic model are compared to the results obtained with the classical random approach.

2 Governing equations

Let us take $u(M,t)$ to denote the displacement of the middle surface of the plate at point M on coordinates (x,y), at time t, and $p(Q,t)$ to denote the acoustic pressure in domain Ω at point Q on coordinates $(x,y,z>0)$, at time t. Adopting the *weak-coupling* assumption discussed in [4], functions $u(M,t)$ and $p(Q,t)$ solve the system of equations presented in [4] and simplified below when there is no membrane tension and a one-sided fluid-loading process:

$$
\begin{aligned}
D\Delta_M^2 u(M,t) + m\frac{\partial^2 u}{\partial t^2}(M,t) = & \\
-f(M,t) - p(M,0,t), \quad \forall M \in \Sigma, & \qquad \text{(a)} \\
\Delta p(Q,t) - \frac{1}{c^2}\frac{\partial^2 p}{\partial t^2}(Q,t) = 0, \quad \forall Q \in \Omega, & \qquad \text{(b)} \\
\rho\frac{\partial^2 u}{\partial t^2}(M,t) + \frac{\partial p}{\partial z}(M,t) = 0, \quad \forall M \in \Sigma, & \qquad \text{(c)} \\
\frac{\partial p}{\partial z}(M,t) = 0, \quad \forall M \in \text{baffle}, & \qquad \text{(d)} \\
\text{Boundary conditions for } u \text{ onto } \partial\Sigma, & \qquad \text{(e)} \\
\text{Radiation conditions for } p. & \qquad \text{(f)}
\end{aligned}
\tag{1}
$$

In the above system of equations, Δ_M^2 is the biharmonic operator calculated with respect to point M which is presented in Appendix A, Δ is the Laplacien operator calculated with respect to variables x, y and z, $D = Eh^3/12(1-\nu^2)$ and h are respectively the bending rigidity and the thickness of the plate. Equation (1-a) is the response of the fluid-loaded plate to the turbulent force $f(M,t)$. The acoustic pressure $p(Q,t)$ obeys the homogeneous d'Alembert equation (1-b) in the fluid domain Ω, the homogeneous Neumann boundary condition (1-d) on the baffle and a condition involving outgoing waves (1-f) at infinity. The acoustic source in Ω is given by the plate acceleration through Equation (1-c). The boundary conditions (1-e) for the displacement of the plate are: **Clamped boundary:** $u = 0$ if $M \in \partial\Sigma$, $\partial_x u = 0$ if $x \in \{0,a\}$, $\partial_y u = 0$ if $y \in \{0,b\}$. **Simply supported boundary:** $u = 0$ if $M \in \partial\Sigma$, $\partial^2_{x^2} u = 0$ if $x \in \{0,a\}$, $\partial^2_{y^2} u = 0$ if $y \in \{0,b\}$. The excitation force $f(M,t)$ due to the turbulent boundary layer is a random field stationary up to order 2 with respect to the time and space variables. The system (1) has no time Fourier transform since the random field $f(M,t)$ has no time Fourier transform [13]. To solve the system (1), let us introduce the Green's kernel $\Gamma(M,M')$ of the displacement of the fluid-loaded plate as the solution to the following system of equations:

$$\begin{aligned} D\Delta_M^2\Gamma(M,M') - m\omega^2\Gamma(M,M') = \\ -\delta_{M'}(M) - P(M,0), \quad \forall M, M' \in \Sigma, \\ \Delta P(Q) + k^2 P(Q) = 0, \quad \forall Q \in \Omega, \\ \frac{\partial P}{\partial z}(M) = \rho\omega^2\Gamma(M,M'), \quad \forall M, M' \in \Sigma, \\ \frac{\partial P}{\partial z}(M) = 0, \quad \forall M \in \text{baffle}, \\ \text{Boundary conditions for } \Gamma(M,M') \text{ when } M \in \partial\Sigma, \\ \text{Sommerfeld radiation conditions for } P. \end{aligned} \tag{2}$$

In system (2), $P(Q)$ is the time Fourier transform of the acoustic pressure $p(Q,t)$, ω is the angular frequency, k is the acoustic wavenumber ($k = \omega/c$), $\delta_{M'}(M)$ is the Dirac delta function at the point M' on coordinates (x', y'): $\delta_{M'}(M) = \delta(x - x') \otimes \delta(y - y')$, where $\otimes$ is the tensor product. In order to simplify the equations, the variable ω will be omitted from the name of the functions $\Gamma(M,M')$ and $P(Q)$. The time-dependent Green's kernel $\gamma(M,M',t)$ of the displacement of the fluid-loaded plate is defined as the inverse time Fourier transform of the Green's kernel $\Gamma(M,M')$:

$$\gamma(M,M',t) = \frac{1}{2\pi}\int_{I\!R} \Gamma(M,M') e^{-\imath\omega t}\, d\omega. \tag{3}$$

The kernel $\gamma(M, M', t)$ gives access to an expression for the displacement of the fluid-loaded plate excited by the random force $f(M, t)$:

$$u(M,t) = \int_{I\!R} \iint_{I\!R^2} \gamma(M, M', t-\tau) f(M', \tau)\ dM'\ d\tau. \tag{4}$$

The displacement $u(M, t)$ defined by Formula (4) is a random field stationary up to order 2 with respect to time.

3 Vibro-acoustic response of the turbulent boundary layer excited panel

A classical spectral analysis of the random field $u(M, t)$ defined by Formula (4) yields the model proposed by Davies [1] in 1971 for the power spectrum $S_u^t(M)$ of the displacement of the turbulent boundary layer excited panel:

$$\begin{aligned} &S_u^t(M) = \\ &\iint_\Sigma \iint_\Sigma \Gamma(M, M') S_f^t(M' - M'') \Gamma^*(M, M'')\ dM'\ dM''. \end{aligned} \tag{5}$$

In the above integral, the function $\Gamma(M, M')$ is the Green's kernel of the displacement of the fluid-loaded plate defined by system (2), $\Gamma^*(M, M')$ denotes the complex conjugate of kernel $\Gamma(M, M')$. The function $S_f^t(M)$ occurring in integral (5) is the power spectrum of the turbulent wall pressure fluctuations $f(M, t)$. Since the random field $f(M, t)$ is stationary up to order 2 with respect to the space variables, its power spectrum $S_f^t(M)$ can be expressed as the inverse space Fourier transform of the wavevector-frequency power spectrum $S_f(K)$ defined by:

$$\begin{aligned} S_f^t(M) &= \frac{1}{(2\pi)^2} \iint_{I\!R^2} S_f(K)\ e^{\imath KM}\ dK, \\ K = (k_x, k_y), &\qquad M = \begin{pmatrix} x \\ y \end{pmatrix}. \end{aligned} \tag{6}$$

In Equation (6), M is the point-vector and K the wavevector. The components k_x and k_y of the wavevector K are the dual variables of the coordinates x and y in a space Fourier transform. When Formula (6) is introduced into the expression (5), the power spectrum of the displacement of the fluid-loaded plate can be written in the form of an integral over the wavevector K:

$$S_u^t(M) = \frac{1}{(2\pi)^2} \iint_{\mathbb{R}^2} U(M,K) S_f(K) U^*(M,K)\, dK. \tag{7}$$

The function $U(M,K)$ which occurs in Formula (7) is the displacement of the fluid-loaded plate when the excitation force is reduced to the contribution of one wavevector K. The function $U(M,K)$ solves the following system of equations:

$$\begin{aligned}
&D\Delta_M^2 U(M,K) - m\omega^2 U(M,K) = \\
&\qquad -e^{-\imath KM} - P(M,0,K), \quad \forall M \in \Sigma, \\
&\Delta P(Q,K) + k^2 P(Q,K) = 0, \quad \forall Q \in \Omega, \\
&\frac{\partial P}{\partial z}(M,K) = \rho\omega^2 U(M,K), \quad \forall M \in \Sigma, \\
&\frac{\partial P}{\partial z}(M,K) = 0, \quad \forall M \in \text{baffle}, \\
&\text{Boundary conditions for } U \text{ onto } \partial\Sigma, \\
&\text{Sommerfeld radiation conditions for } P.
\end{aligned} \tag{8}$$

The power spectrum $S_p^t(M)$ of the acoustic pressure in the fluid domain Ω can be expressed in a similar mathematical form to that of Equation (7):

$$S_p^t(M) = \frac{1}{(2\pi)^2} \iint_{\mathbb{R}^2} P(M,K) S_f(K) P^*(M,K)\, dK. \tag{9}$$

The function $P(M,K)$ occurring in Formula (9) solves de system (8), it can be calculated by using the Green's representation formula for the acoustic pressure:

$$P(M,K) = -\rho\omega^2 \iint_\Sigma G(M,M')U(M',K)\, dM', \tag{10}$$

where $G(M,M')$ is the Green's kernel of the Helmholtz equation satisfying the homogeneous Neumann boundary condition on the $z = 0$ plane, which is obtained from the Green's kernel of the Helmholtz equation using an imaging method. The function $P(M,K)$ is the acoustic pressure radiated at point M when the plate is excited by a single wavevector K.

In [7], the authors used a finite difference method to solve a beam equation coupled with both a fluid cavity and a semi-infinite fluid domain. An other application of the finite difference method to solving a plate equation can also be found in [14]. In the present article, the system of equations (8) is solved by using the order 12 central finite difference scheme given in Appendix A to compute the plate operator, and the integral representation (10) to compute the acoustic pressure in the fluid domain.

4 The wall pressure fluctuations model

The literature provides a large amount of models for the wall pressure fluctuations in a turbulent boundary layer developed over a rigid plane smooth surface. One of the first models was developed by Corcos [15]. Corcos developed an empirical model in which the cross-correlation function of the wall pressure fluctuations is approximated by an exponential behaviour. The Corcos wavevector-frequency power spectrum can be expressed as follows:

$$
\begin{aligned}
S_f(K) = \Phi_0 \left[\alpha\beta\left(\omega/V_c\right)^2\right] \\
/ \left\{\pi^2\left[\left(k_x - \omega/V_c\right)^2 + \left(\alpha\omega/V_c\right)^2\right]\left[k_y^2 + \left(\beta\omega/V_c\right)^2\right]\right\}.
\end{aligned}
\tag{11}
$$

A broad band model for the point power spectrum Φ_0 is:

$$
\Phi_0 = a_+ \left(1 + \gamma\right) \rho_e \nu_*^4/\omega.
$$

The value of the constants in this Corcos model are $\alpha = 0.09$, $\beta = 7\alpha$, $a_+ = 0.766$ and $\gamma = 0.389$. The convective velocity V_c is taken to be equal to $0.7V$. The friction velocity is simply taken to be equal to $\nu_* = 0.03V$. Note that some more sophisticated larger band expressions for the point power spectrum Φ_0 are avialable in the literature [11]. Several turbulent boundary layer models, with various levels of validity, have also been drawn up in the wavevector-frequency domain [16, 17, 18, 19]. Their respective effects on the vibro-acoustic response of an elastic panel are analysed in a paper by Graham [20]. However, studying the turbulence model is not within the scope of the present paper.

The test case presented in the present paper is representative of underwater acoustic problems arising due to the flow induced noise on the antenna of a towed SONAR. The structure is the elastic panel the characteristics of which are presented in Appendix A. The fluid is water, $\rho = 1000\,Kgm^{-3}$, $c = 1500\,ms^{-1}$. The free-stream velocity is $V = 10\,ms^{-1}$. The Corcos model (11) used for this test case is plotted in Figure 2.

5 Wavenumber filtering by a thin elastic plate

Wavevector integration models (7, 9) can be used to represent the plate in the form of a wavevector filter. Let us define the wavevector transfer function of the displacement of the plate at point M by:

$$H_M : K \longrightarrow U(M,K)U^*(M,K). \tag{12}$$

The function $H_M(K)$ gives the wavevector filtering effect of the plate. Now, let us consider the wavevector density function of the displacement of the plate at point M, defined as follows:

$$D_M : K \longrightarrow U(M,K)S_f(K)U^*(M,K). \tag{13}$$

The function $D_M(K)$ gives the contribution of the wavevector K to the displacement of the plate at point M. Figure 3 gives the wavevector density function $D_M(K)$ and the transfer function $H_M(K)$ of the displacement in the middle of the plate at the frequency 133 Hz, which for convenience have been plotted for $k_y = 0$. The wavevector transfer function of the displacement has a major lobe at the origin. This behaviour, which is also shown in [2, 3, 8], indicates that the main contribution to the power spectrum of the displacement of the plate (7) is due to the low wavenumber region of the turbulent wall pressure fluctuations spectrum. From Figure 3, it can be seen that the wavevector density function (13) shows a second peak in the region of the convective wavenumbers. This peak can make a non negligible contribution to the vibro-acoustic response of the plate at high flow speeds [20]. Figure 4 illustrates the importance of the effects of the low wavenumber region on the displacement of the plate. It gives the power spectrum of the acceleration in the middle of the plate calculated using Formula (7) when the wavenumber integration domain in the direction k_x is increased from the acoustic domain ($k_x = k = \omega/c$) to the convective domain ($k_x = \omega/V_c$) of the turbulent boundary layer power spectrum $S_f(K)$. Figure 4 shows that the wavevector integral (7) converges rapidly and that the contribution of the wavenumbers k_x greater than $50\,k$ in terms of their absolute value to the displacement of the plate is negligible. Therefore, as far as subsonic applications are concerned, and for panels with similar mechanical properties to that used in the present study, the effect of the wavenumbers located in the region of the convective peak on the response of the structure can be neglected. Similar results for the wavenumber filtering of the turbulent excitation by a rectangular panel are presented in [8] in the case of a clamped plate.

6 Deterministic approximation of the random model

Computing the vibro-acoustic responses of the structure using Formulae (7, 9) involves integrating the wavevector density function plotted in Figure 3. Since this function oscillates rapidly, the calculation will be highly time consuming if one attempts to compute an accurate integration. In this section, an approximate model based on a deterministic approach is proposed. The function $U(M, K)$ which features in the definition of the power spectrum (7) is the displacement of the fluid-loaded plate when the excitation force reduces to the contribution of one wavevector. Consider a simply supported plate *in vacuo*. A classical modal approach yields an expression for the displacement $U(M,K)$ in the form of a series of eigenmodes $W_{mn}(M)$ of the *in vacuo* simply supported panel:

$$U(M,K) = \frac{1}{D} \sum_{m=1}^{N} \sum_{n=1}^{N} \frac{\left(W_{mn}(M), e^{\imath KM}\right)}{\lambda_{mn}^4 - \lambda^4} W_{mn}(M). \tag{14}$$

In the above equation, N is the number of modes taking part in the response of the structure, the value of which will be discussed below, $\lambda^2 = \sqrt{m\omega^2/D}$ is an elastic wavenumber, and λ_{mn}, f_{mn} and $W_{mn}(M)$ are respectively the eigenvalues, the eigenfrequencies and the normalized eigenmodes of the simply supported panel *in vacuo*:

$$\begin{aligned} \lambda_{mn}^2 &= \left(\frac{m\pi}{a}\right)^2 + \left(\frac{n\pi}{b}\right)^2, \\ W_{mn}(x,y) &= \frac{2}{\sqrt{ab}} \sin\left(\frac{m\pi}{a} x\right) \sin\left(\frac{n\pi}{b} y\right) \\ f_{mn} &= \frac{1}{2\pi} \sqrt{D/m}\, \lambda_{mn}^2 \end{aligned} \tag{15}$$

When calculating the displacement of a plate *in vacuo* using Formula (14), some internal dissipation must be introduced into the model. This structural damping can take the form of a small imaginary component in the bending rigidity of the plate $D = (1 - \imath\eta(\omega))Eh^3/12(1-\nu^2)$ where $\eta(\omega) > 0$ is the material loss factor. Then, the eigenvalues λ_{mn} become complex, and the sum (14) is always defined. In this study, we never need to compute the modal series (14). In order to simplify the discussion, details are therefore given for the case where $\eta(\omega) = 0$. The modal excitation term is equal to:

$$\left(W_{mn}(M), e^{\imath KM}\right) = \iint_{\Sigma} W_{mn}(M) e^{\imath KM} dM. \tag{16}$$

When the series (14) is introduced into the power spectrum of the displacement (7), one obtains:

$$S_u^t(M) = \frac{1}{(2\pi)^2} \cdot \iint_{R^2} \left| \frac{1}{D} \sum_{m=1}^{N} \sum_{n=1}^{N} \frac{\left(W_{mn}(M), e^{\imath KM}\right)}{\lambda_{mn}^4 - \lambda^4} W_{mn}(M) \sqrt{S_f(K)} \right|^2 dK. \tag{17}$$

The function occurring inside the modulus in Formula (17) is the wavevector density function of the displacement defined by Formula (13), which is plotted in Figure 3. Since this function decreases rapidly as $|K|$ increases, the main contributions to the double integral in Formula (17) are due the wavevectors which are in a region very close to the origin. This behaviour of the function $D_M(K)$ makes it possible to transform the infinite integral in Formula (17) into an integral over a bounded domain $[k_{x_1}, k_{x_2}] \times [k_{y_1}, k_{y_2}]$. The values of the bounds k_{x_1}, k_{x_2}, k_{y_1} and k_{y_2} result from the study of the function $D_M(K)$. A classical Riemann integration rule is used to express the double integral in Formula (17) in the form of a double sum:

$$S_u^t(M) = \frac{\Delta k_x \, \Delta k_y}{(2\pi)^2} \sum_{i=-N}^{N} \sum_{j=-N}^{N} \left| \frac{1}{D} \sum_{m=1}^{N} \sum_{n=1}^{N} \frac{\left(W_{mn}(M), e^{\imath K_{ij} M}\right)}{\lambda_{mn}^4 - \lambda^4} \sqrt{S_f(K_{ij})} W_{mn}(M) \right|^2 , \tag{18}$$

where the constants Δk_x and Δk_y are the integration steps in directions k_x and k_y. The number N used in the discrete integration procedure (18) is taken to be equal to the number of modes appearing in the response of the structure in Equation (14). In [1] the author suggested that the displacement of the fluid-loaded plate may be mainly governed by the wavevectors of the turbulent excitation which show a good match with the mode shapes of the plate. Under the same assumption, the wavevectors K_{ij} in Formula (18) are taken to be equal to the elastic wavenumbers appearing in the definition (15) of the eigenmodes $W_{mn}(M)$:

$$\begin{aligned} K_{ij} &= \left(\frac{i\pi}{a}, \frac{j\pi}{b}\right) \quad i, j = -N, ... -1, 0, 1, ..., N, \\ &\Longrightarrow \Delta k_x = \frac{\pi}{a}, \quad \Delta k_y = \frac{\pi}{b}. \end{aligned} \tag{19}$$

A few calculations, details of which are given in Appendix B, leads to the following approximation for the modal excitation term (16):

$$\left(W_{mn}(M), e^{\imath K_{ij} M}\right) \simeq -\frac{\sqrt{ab}}{2} \operatorname{sgn}(i) \operatorname{sgn}(j) \delta_{|i|}^{m} \delta_{|j|}^{n}, \tag{20}$$

where $\delta_{|i|}^{m}$ is the Kronecker delta symbol defined by $\delta_{|i|}^{m} = 1$ if $m = |i|$ and $\delta_{|i|}^{m} = 0$ if $m \neq |i|$. When the excitation term (20) is introduced into the series (18), the power spectrum (18) can be approximated, as shown in Appendix B, in the following form:

$$\begin{aligned} S_u^t(M) \simeq & \left| \frac{1}{D} \sum_{m=1}^{N} \sum_{n=1}^{N} \right. \\ & \left. \frac{\left(W_{mn}(M), \frac{1}{8} \sum_{i=-N}^{N} \sum_{j=-N}^{N} \sqrt{S_f(K_{ij})} W_{|i||j|}(M)\right)}{\lambda_{mn}^4 - \lambda^4} W_{mn}(M) \right|^2 \end{aligned} \tag{21}$$

The approximate power density function expressed in the above formula is equivalent to the square of the modulus of the displacement of the *in vacuo* panel excited by the following deterministic force:

$$\frac{1}{8} \sum_{i=-N}^{N} \sum_{j=-N}^{N} \sqrt{S_f(K_{ij})} W_{|i||j|}(M). \tag{22}$$

When calculating a broad-band response of the plate using the above deterministic excitation force, the number N determining the number of wavevectors taking part in the turbulent excitation must be greater than the number of modes involved in the response of the structure. However, since the error made in the excitation term (22), due to the approximation (20), increases with the number N, it is worth including only a small number wavevectors in Formula (22). The approach proposed in the present study consists in using a weight function to reduce the influence of the wavevectors that do not show a good match with the mode shape of the plate at the frequency of interest. This weighted model for the turbulent excitation force is:

$$F_{TBL}(M) = \frac{1}{8} \sum_{i=-N}^{N} \sum_{j=-N}^{N} e^{-\frac{\left|f-f_{ij}\right|}{\sigma}} \sqrt{S_f(K_{ij})} W_{|i||j|}(M), \tag{23}$$

where f is the frequency, f_{ij} is the eigenfrequency of the mode (i, j), and σ is a number determining the number of wavevectors taking part in the turbulent excitation. In the present numerical experiment, we used $\sigma = 500$, and since we consider a simply supported panel, the f_{ij} are given by Formula (15).

Let us now consider a panel coupled with an infinite fluid domain. The eigenvalues and the eigenmodes of the fluid-loaded plate can be calculated numerically, and as shown in [22], these eigenvalues are complex and possess a negative imaginary part. However, computing the complex eigenvalues and eigenmodes of a fluid-loaded plate is not an easy task. The method proposed here for computing the numerical simulations is based on the assumption that, as long as the mode shapes of the fluid-loaded panel are not significantly different from the mode shapes of the *in vacuo* plate, which is true when dealing with structures which are rigid enough, the model presented for an *in vacuo* plate will apply when the plate is coupled with a fluid domain. The deterministic force

(23) is now introduced into a time harmonic model solving the vibro-acoustic responses $u(M)$ and $p(M)$ of an elastic panel coupled with a fluid domain. The governing system of equations for this deterministic model is expressed below:

$$\begin{aligned} & D\Delta_M^2 u(M) - m\omega^2 u(M) = \\ & -F_{TBL}(M) - p(M,0), \quad \forall M \in \Sigma, && \text{(a)} \\ & \Delta p(Q) + k^2 p(Q) = 0, \quad \forall Q \in \Omega, && \text{(b)} \\ & \frac{\partial p}{\partial z}(M) = \rho\omega^2 u(M), \quad \forall M \in \Sigma, && \text{(c)} \\ & \frac{\partial p}{\partial z}(M) = 0, \quad \forall M \in \text{baffle}, && \text{(d)} \\ & \text{Boundary conditions for } u \text{ onto } \partial\Sigma, && \text{(e)} \\ & \text{Sommerfeld radiation conditions for } p. && \text{(f)} \end{aligned} \tag{24}$$

The approximate power spectrum for the displacement of the plate (7), which is given by Formula (21), therefore reduces to:

$$S_u^t(M) \simeq |u(M)|^2 \tag{25}$$

The approximate power spectrum for the acoustic pressure radiated by the turbulent boundary layer excited panel (9) can be expressed in the same mathematical form:

$$S_p^t(M) \simeq |p(M)|^2 \tag{26}$$

The functions $u(M)$ and $p(M)$ occurring in Formulae (25) and (26) are respectively the displacement and the acoustic radiation of the fluid-loaded plate Σ subjected to the deterministic force $F_{TBL}(M)$ defined by Equation (23). These functions $u(M)$ and $p(M)$ can be calculated by solving the system of equations (24).

7 Test cases

As a preamble to these test-cases, a grid refinement study was performed to ensure that the plate equation used in both the exact (7-10) and approximate (23-26) models was correctly solved. Figure 5 shows the displacement of the plate at point (0.33m, 0.33m), calculated by solving the plate equation (24-a) using the order 12 finite difference scheme given in Appendix A. The results obtained with both the $[13 \times 19]$ and the $[25 \times 37]$ mesh-grids were identical and the two curves are superimposed, while the curve obtained with the last mesh-grid, $[7 \times 10]$ is slightly different. It can be clearly seen from Figure 5 that, as far as the displacement of the plate is concerned, the mesh-grid $[13 \times 19]$ is satisfactory.

Three test cases were computed. In the first two cases, the influence of the fluid was neglected: In the first case a simply supported plate *in vaccuo* was studied, and in the second case a clamped plate *in vaccuo*. The third test case dealt with a *heavy-fluid* loading: a simply supported plate is coupled on one side with a water domain.

Figures 6 and 7 give the power spectrum of the acceleration of the turbulent boundary layer excited panel when the fluid loading is neglected. The displacement is calculated at the point $(0.33\,m, 0.46\,m)$ using the usual random approach (7) and using the deterministic model (25) in which the turbulent excitation force is introduced in the form of Formula (23) where the number N is taken to be equal to 50. Figure 6 gives the results obtained in the case of a simply supported panel. Figure 7 gives the results obtained in the case of a clamped plate. In this latter study, the eigenfrequencies f_{ij} of the clamped plate were estimated numerically using the method proposed in [21], and the associated eigenmodes $W_{ij}(M)$ were approximated by the eigenmodes of the simply supported panel defined by Formula (15). Apart from the *anti-resonance* frequencies, the results of the deterministic model showed a very good match with those obtained with the random approach. In particular, the amplitudes of the resonant peaks are well described.

The deterministic model (23) for the turbulent excitation force was applied to the calculation of the vibro-acoustic response of a panel immersed on one side in a semi-infinite water domain. In this model, the eigenfrequencies f_{ij} of the fluid-loaded plate are calculated by computing the minima of the spectrum of the determinant of system (2) when $\omega \in I\!R$ and the corresponding eigenmodes W_{ij} are approximated by the eigenmodes of the simply supported plate *in vaccuo* which are defined by Formula (15). In Figure 8, the approximation (25) of the power spectrum of the acceleration of the simply supported panel is compared to the power spectrum calculated with the exact model (7). Figure 9 compares the acoustic pressures at the point $(0.33\,m, 0.46\,m, 0.5\,m)$ obtained with both the deterministic approximation (26) and the exact random model (9). Although the comparison between the displacements presented in Figure 8 were satisfactory, excepted at the *anti-resonance* frequencies, the results presented for the acoustic pressure in Figure 9 were less convincing. A second problem certainly arrises due to the use of a high order finite difference method to solve the plate equation. The meshing of the plate is therefore poor, and it follows that the integral (10) expressing the acoustic pressure was not estimated properly.

8 Conclusion

A deterministic model based on an analytical wavenumber integration procedure is proposed here for predicting both the displacement and the acoustic radiation of an elastic rectangular plane panel subjected to clamped or simply supported boundary conditions and excited by a turbulent flow of fluid at low Mach number. The results obtained with this deterministic model are compared with those obtained with the classical random approach. In this numerical study, good agreement was observed between the results obtained with the two approaches. The main advantage of this deterministic model lies in the CPU saving to which it leads because the random approach involves solving a large number of elasto-acoustic problems (8) per frequency in order to be able to calculate the power spectrums given by the integrals (7) and (9); whereas, the deterministic approximations of these functions given by Formulae (25) and (26) can be calculated by solving a single fluid-structure problem (24) per frequency. Moreover, problems (8) and (24) amount to approximately the same numerical effort because they differ only in the excitation term: in (8), the excitation term is given by one wavevector, and in (24) the excitation term contains several wavevectors. In the test case considered here, the computation of the deterministic models (25, 26) makes for significant savings because it is approximatly 50 time faster than the random approaches (7, 9). The behaviour assumed in the hypothesis that the subconvective region of the turbulent wavevector-frequency power spectrum greatly affects the vibro-acoustic response of the system was confirmed in a numerical study on a low Mach number water flow. In [8], similar behaviour was observed in a subsonic (Mach number $\simeq 0.5$) air flow, and there is therefore no doubt that the deterministic model described in the present study also applies in air.

References

[1] H. G. Davies 1971. *Journal of the Acoustical Society of America*, 49:878–889, 1971. Sound from turbulent-boundary-layer-excited panels.

[2] N. C. Martin and P. Leehey. *Journal of Sound and Vibration*, 52(1):95–120, 1977. Low wavenumber wall pressure measurements using a rectangular membrane as a spatial filter.

[3] Y. F. Hwang and G. Maidanik 1990. *Journal of Sound and Vibration*, 142:135–152, 1990. A wavenumber analysis of the coupling of a structural mode and flow turbulence.

[4] W. R. Graham 1996. *Journal of Sound and Vibration*, 192:101–120, 1996. Boundary layer induced noise in aircraft, part I: the flat plate model.

[5] W. R. Graham 1996. *Journal of Sound and Vibration*, 192:121–138, 1996. Boundary layer induced noise in aircraft, part II: the trimmed flat plate model.

[6] W. R. Graham 1998. *Proceedings of the Royal Society of London*, 454:111–137, 1998. The effect of mean flow on the radiation efficiency of rectangular plates.

[7] D. Mazzoni and U. Kristiansen 1999. *Flow, Turbulence and Combustion*, 61:133–159, 1999. Finite difference method for the acoustic radiation of an elastic plate excited by a turbulent boundary layer: A spectral domain solution.

[8] C. Maury, P. Gardonio and S. J. Elliott, 2002. *Journal of Sound and Vibration*, to appear. A wavenumber approach to modelling the response of a randomly excited panel, part I: General theory.

[9] . D. G. Crighton, A. P. Dowling, J. E. Ffowcs Williams, M. Heckl and F. G. Leppington, 1992. *Modern methods in analytical acoustics, lecture notes.* Berlin: Springer-Verlag.

[10] G. Robert 1984. Thèse, Ecole Centrale de Lyon, 36 avenue Guy Collongue, B.p. 163, 69131 ECULLY, FRANCE (réf. E.C.L. 84–02). *Modélisation et Simulation Du Champ Excitateur Induit sur Une Structure Par Une Couche Limite Turbulente.*

[11] S. Bano, R. Marney, L. Jourdan and J.-P. Guibergia 1992. *Journal d'Acoustique*, 5:99–124, 1992 Etude théorique et expérimentale de la réponse vibro-acoustique d'une plaque couplée â une cavité en fluide lourd.

[12] C. Maury, P. Gardonio and S. J. Elliott, 2002. *Journal of Sound and Vibration*, to appear. A wavenumber approach to modelling the response of a randomly excited panel, part II: Application to aircraft panels excited by a turbulent boundary layer.

[13] M. B. Priestley 1981. Academic Press, London, 1981. *Spectral Analysis And Time Series.*

[14] G. Aksu and R. Ali 1976. *Journal of Sound and Vibration*, 48:15–25, 1976. Free vibrations analysis of stiffened plates using finite difference method.

[15] G. M. Corcos 1963. *Journal of the Acoustical Society of America*, 35:192–199, 1963. Resolution of pressure in turbulence.

[16] D. M. Chase 1980 *Journal of Sound and Vibration* 70, 29-67. Modeling the wavevector-frequency spectrum of turbulent boundary layer wall pressure.

[17] J. E. Ffowcs Williams 1982 *Journal of Fluid Mechanics* 125, 9-25. Boundary-layer pressures and the Corcos model: a development to incorporate low-wavenumber constraint.

[18] D.M. Chase 1987 *Journal of Sound and Vibration* 112, 125-147. The character of the turbulent wall pressure spectrum at subconvective wavenumbers and a suggested comprehensive model.

[19] D.M. Chase 1990 *Journal of the Acoustical Society of America* 90(2), 1032-1040. The wave-vector-frequency spectrum of pressure on a smooth plane in turbulent boundary layer flow at low Mach number.

[20] W. R. Graham 1997. *Journal of Sound and Vibration*, 206(4):541–565, 1997. A comparison of models for the wavenumber-frequency spectrum of turbulent boundary layer pressures.

[21] A. W. Leissa 1973. *Journal of Sound and Vibrations*, 31:257–293, 1973. The free vibration of rectangular plates.

[22] P. J. T. Filippi and D. Mazzoni 1997. In Ayyub Haldar, Guran, editors, *Uncertainty Modeling in Finite Element, Fatigue and Stability of Structures (Series on Stability, Vibrations and Control of Systems, Vol. 9)*, 117–158, WorldScientific 1997. Response of a vibrating structure to a turbulent wall pressure: Fluid-loaded structure modes series and boundary element method.

Appendix A

Order 12 finite difference scheme for the biharmonic operator

This appendix gives the order 12 central finite difference scheme for the biharmonic operator. Since we did not want to restrict this scheme to certain aspect ratio of the plate ($L_x/L_y = \alpha/\beta$, with α, $\beta \in I\!N$), the finite difference scheme was computed with different steps in the directions x and y. Let us take $U_{i,j}$ to denote the displacement of the plate at point (x_i, y_j) on the mesh-grid. The order 12 central finite difference scheme for the biharmonic operator is expressed by the following formula:

$$\Delta^2 U = \frac{\partial^4 U}{\partial x^4} + 2\frac{\partial^4 U}{\partial x^2 \partial y^2} + \frac{\partial^4 U}{\partial y^4},$$

$$U(x_i, y_j) = U_{i,j},$$

$$\Delta^2 U_{i,j} = \sum_{m=-7}^{7} \sum_{n=-7}^{7} \alpha_{m,n} U_{i+m,j+n}.$$

where the $\alpha_{m,n}$ are constants given in the table below:

$$\alpha_{0,0} = \frac{28231}{1620}\frac{1}{dx^2dy^2} + \frac{54613}{3780}\frac{1}{dx^4} + \frac{54613}{3780}\frac{1}{dy^4}$$

$$\alpha_{0,1} = -\frac{125173}{12600}\frac{1}{dx^2dy^2} - \frac{90281}{8400}\frac{1}{dy^4} \qquad \alpha_{0,2} = \frac{36521}{25200}\frac{1}{dx^2dy^2} + \frac{222581}{50400}\frac{1}{dy^4}$$

$$\alpha_{0,3} = -\frac{6018}{22680}\frac{1}{dx^2dy^2} - \frac{247081}{226800}\frac{1}{dy^4} \qquad \alpha_{0,4} = \frac{209}{5040}\frac{1}{dx^2dy^2} + \frac{31957}{138600}\frac{1}{dy^4}$$

$$\alpha_{0,5} = -\frac{31}{6930}\frac{1}{dx^2dy^2} - \frac{2077}{55440}\frac{1}{dy^4} \qquad \alpha_{0,6} = \frac{1}{4158}\frac{1}{dx^2dy^2} + \frac{20137}{4989600}\frac{1}{dy^4}$$

$$\alpha_{0,7} = -\frac{59}{277200}\frac{1}{dy^4} \qquad \alpha_{1,1} = \frac{3557}{630}\frac{1}{dx^2dy^2} \qquad \alpha_{1,2} = -\frac{361}{450}\frac{1}{dx^2dy^2}$$

$$\alpha_{1,3} = \frac{193}{1350}\frac{1}{dx^2dy^2} \qquad \alpha_{1,4} = -\frac{47}{2160}\frac{1}{dx^2dy^2} \qquad \alpha_{1,5} = \frac{17}{7425}\frac{1}{dx^2dy^2}$$

$$\alpha_{1,6} = -\frac{1}{8316}\frac{1}{dx^2dy^2} \qquad \alpha_{2,2} = \frac{221}{2520}\frac{1}{dx^2dy^2} \qquad \alpha_{2,3} = -\frac{1}{90}\frac{1}{dx^2dy^2}$$

$$\alpha_{2,4} = \frac{23}{21600}\frac{1}{dx^2dy^2} \qquad \alpha_{2,5} = -\frac{1}{18900}\frac{1}{dx^2dy^2} \qquad \alpha_{3,3} = \frac{1}{1134}\frac{1}{dx^2dy^2}$$

$$\alpha_{3,4} = -\frac{1}{25200}\frac{1}{dx^2dy^2}$$

The missing $\alpha_{m,n}$ can be calculated by using the following rules:

$$\alpha_{-m,n} = \alpha_{m,-n} = \alpha_{m,n}, \quad \alpha_{m,n}(dx, dy) = \alpha_{n,m}(dy, dx), \quad \text{if } (m+n) > 7 \text{ then } \alpha_{m,n} = 0.$$

The numerical performance of this scheme was tested in terms of the accuracy with which the eigenfrequencies of a simply supported rectangular plate *in vacuo* were determined. The geometry and the mechanical properties of the panel tested were:

$$\begin{aligned} \text{length}: &\quad a = 0.5\,m \\ \text{width}: &\quad b = 0.75\,m \\ \text{thickness}: &\quad h = 0.005\,m \\ \text{Young's modulus}: &\quad E = 210^{11}\,Nm \\ \text{Poisson ratio}: &\quad \nu = 0.3 \\ \text{mass per unit area}: &\quad m = 7800 \cdot e\ Kgm^{-2} \\ \text{mesh-grid}: &\quad 13 \times 19 \text{ points} \end{aligned}$$

The following table compares the resonance frequencies of the simply supported plate *in vacuo* calculated with the order 4, 6, 8, 10 and 12 finite difference schemes with the resonance frequencies obtained by performing a classical analytical calculation [21]:

Numerical dispersion of order 4, 6, 8, 10, 12 finite difference schemes

mode	Y sampling (points per wavelength)	resonance frequencies (Hz)					
		analytical calculation	finite difference method				
			order 4	order 6	order 8	order 10	order 12
(1, 1)	35	69.54	69.5	69.5	69.5	69.5	69.5
Error (%)			0	0	0	0	0
(1, 2)	18	133.72	133.7	133.7	133.7	133.7	133.7
Error (%)			0	0	0	0	0
(2, 2)	18	278.14	277.9	278.1	278.1	278.1	278.1
Error (%)			0	0	0	0	0
(1, 3)	12	240.7	240.5	240.7	240.7	240.7	240.7
Error (%)			∼0	0	0	0	0
(3, 3)	12	625.82	623.5	625.6	625.8	625.8	625.8
Error (%)			0.4	∼0	0	0	0
(1, 4)	9	390.47	389.4	390.4	390.5	390.5	390.5
Error (%)			0.3	∼0	0	0	0
(4, 4)	9	1112.57	1100.1	1110.4	1112.2	1112.5	1112.6
Error (%)			1.1	0.2	∼0	∼0	0
(1, 5)	7	583.03	579.0	582.5	583.0	583.0	583.0
Error (%)			0.7	∼0	0	0	0
(5, 5)	7	1738.39	1694.1	1726.9	1735.2	1737.4	1738.1
Error (%)			2.5	0.7	0.2	∼0	∼0
(1, 6)	6	818.38	806.9	816.3	818.0	818.3	818.4
Error (%)			1.4	0.2	∼0	0	0
(1, 7)	5	1096.52	1069.0	1089.8	1094.8	1096.1	1096.4
Error (%)			2.5	0.6	0.1	∼0	0
(1, 8)	4.6	1417.46	1359.4	1399.6	1411.7	1415.5	1416.8
Error (%)			4.0	1.3	0.4	0.1	∼0

Appendix B

Evaluation of the turbulent excitation term

In this Appendix, the turbulent excitation term involved in Formula (18) is calculated:

$$\begin{aligned}\left(W_{mn}(M), e^{\imath K_{ij}M}\right) = & \frac{2}{\sqrt{ab}}\left(\int_0^a \sin\left(\tfrac{m\pi}{a}x\right) e^{\imath\frac{i\pi}{a}x}dx\right) \\ \cdot & \left(\int_0^b \sin\left(\tfrac{n\pi}{b}y\right) e^{\imath\frac{j\pi}{b}y}dy\right)\end{aligned} \qquad B1$$

The first term in brackets expands as follows:

$$\begin{aligned}\int_0^a \sin\left(\tfrac{m\pi}{a}x\right) e^{\imath\frac{i\pi}{a}x}dx = & \int_0^a \sin\left(\tfrac{m\pi}{a}x\right)\cos\left(\tfrac{i\pi}{a}x\right)dx \\ + & \ \imath\int_0^a \sin\left(\tfrac{m\pi}{a}x\right)\sin\left(\tfrac{i\pi}{a}x\right)dx.\end{aligned} \qquad B2$$

The real part of the above formula is equal to:

$$\int_0^a \sin\left(\frac{m\pi}{a}x\right)\cos\left(\frac{i\pi}{a}x\right)dx = \frac{a}{\pi}\frac{m}{m^2-i^2}\left[1-(-1)^{m+i}\right]\overline{\delta}_{|i|}^m, \qquad B3$$

where the symbol $\overline{\delta}_i^m$ is defined by $\overline{\delta}_i^m = 1$ if $i \neq m$ and $\overline{\delta}_i^m = 0$ if $i = m$. The imaginary part of Formula (B2) can be written:

$$\int_0^a \sin\left(\frac{m\pi}{a}x\right)\sin\left(\frac{i\pi}{a}x\right)dx = \frac{a}{2}\,\mathrm{sgn}(i)\,\delta_{|i|}^m, \qquad B4$$

where δ_i^m is the Kronecker delta symbol. Formulae (B3, B4) yield an expression for the modal excitation term (B1):

$$\begin{aligned}(W_{m,n}(M), e^{\imath K_{i,j}M}) = & -\frac{\sqrt{ab}}{2}\,\mathrm{sgn}(i)\,\mathrm{sgn}(j)\,\delta_{|i|}^m\,\delta_{|j|}^n && \text{(a)} \\ +\frac{2\sqrt{ab}}{\pi^2}\frac{m}{m^2-i^2}\frac{n}{n^2-j^2} & \left[1-(-1)^{m+i}\right]\left[1-(-1)^{n+j}\right]\overline{\delta}_{|i|}^m\,\overline{\delta}_{|j|}^n && \text{(b)} \\ & +\imath\frac{\sqrt{ab}}{\pi}\frac{m}{m^2-i^2}\left[1-(-1)^{m+i}\right]\mathrm{sgn}(j)\,\delta_{|j|}^n\,\overline{\delta}_{|i|}^m && \text{(c)} \\ & +\imath\frac{\sqrt{ab}}{\pi}\frac{n}{n^2-j^2}\left[1-(-1)^{n+j}\right]\mathrm{sgn}(i)\,\delta_{|i|}^m\,\overline{\delta}_{|j|}^n && \text{(d)}\end{aligned} \qquad B5$$

Assuming now that the response of the mechanical system is mainly due to the resonant modes and that the resonance frequencies in the panel are widely separated, we are interested in determining the value of the power spectrum of the displacement (18) at the resonance frequency of a structural mode (m, n) satisfying $(m < N)$ and $(n < N)$. Under the assumption that the vibro-acoustic response of the plate is mainly governed by the wavevectors which show a good match with the mode (m, n), the summation in Equation (B5) mainly involves the term (a) and the contribution of the terms (b), (c) and (d) can be neglected. Therefore, the modal excitation can be approximated by Formula (20). Introducing Equation (20) into the series (18) yields:

$$S_u^t(M) \simeq \sum_{i=-N}^{N} \sum_{j=-N}^{N} \left| \frac{1}{4D} \frac{\sqrt{S_f(K_{ij})}}{\lambda_{ij}^4 - \lambda^4} \operatorname{sgn}(i) \operatorname{sgn}(j) \, W_{|i||j|}(M) \right|^2 . \qquad B6$$

The wavevector-frequency power spectrum of the wall pressure fluctuations satisfies the following condition:

$$S_f(K_{ij}) = S_f(K_{i(-j)}). \qquad B7$$

Under the assumption that the low wavenumber region of the wavevector-frequency power spectrum of the turbulent excitation contributes mainly to the displacement of the plate, in this region one can write:

$$S_f(K_{ij}) \simeq S_f(K_{(-i)j}). \qquad B8$$

Upon introducing Formula (B7) and assumption (B8) into Formula (B6), the power spectrum of the displacement of the plate simplifies into:

$$S_u^t(M) \simeq \sum_{i=1}^{N} \sum_{j=1}^{N} \left| \frac{1}{2D} \frac{\sqrt{S_f(K_{ij})}}{\lambda_{ij}^4 - \lambda^4} W_{ij}(M) \right|^2 . \qquad B9$$

Since we calculated the power spectrum of the displacement at the resonance frequency of the mode (m, n), and since the resonance frequencies of the panel are widely separated, (m, n) is the only effective term in the summation (B9). Accordingly, the power spectrum of the displacement can be approximated by:

$$S_u^t(M) \simeq \left| \frac{1}{2D} \sum_{i=1}^{N} \sum_{j=1}^{N} \frac{\sqrt{S_f(K_{ij})}}{\lambda_{ij}^4 - \lambda^4} W_{ij}(M) \right|^2, \qquad B10$$

The above formula includes only the wavevectors with positive components. The negative components of the wavevectors are re-introduced into the model (B10) by including the assumptions (B7, B8). This yields the Formula (21).

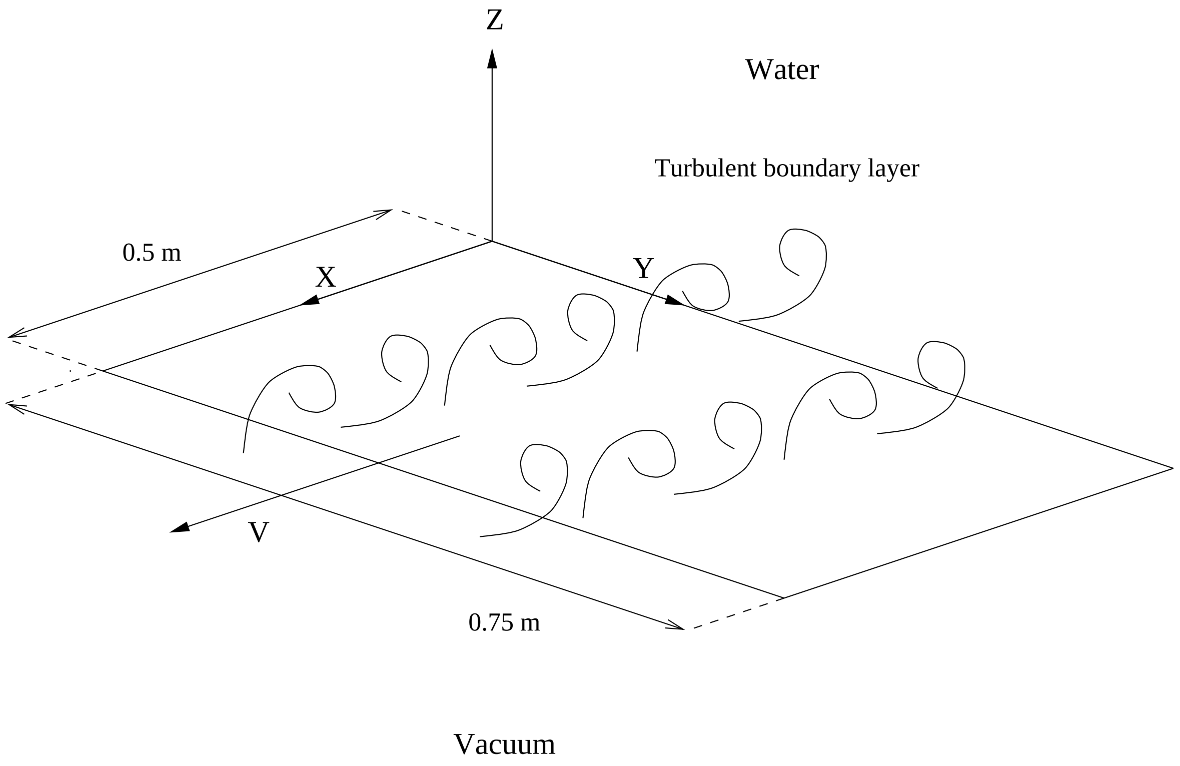
Z
Water
Turbulent boundary layer
0.5 m
X
Y
V
0.75 m
Vacuum

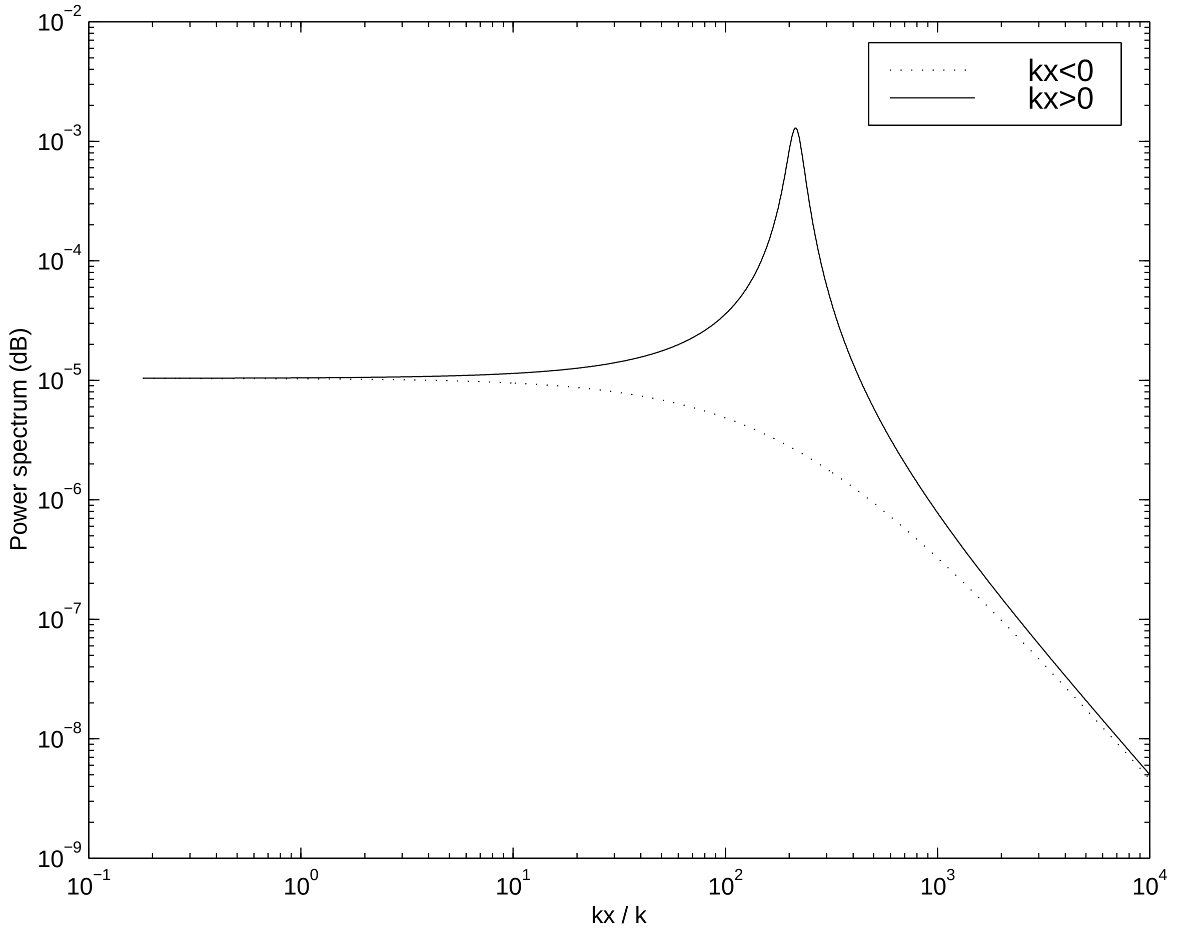

kx<0
kx>0
Power spectrum (dB)
kx / k
10^{-2}
10^{-3}
10^{-4}
10^{-5}
10^{-6}
10^{-7}
10^{-8}
10^{-9}
10^{-1}
10^{0}
10^{1}
10^{2}
10^{3}
10^{4}

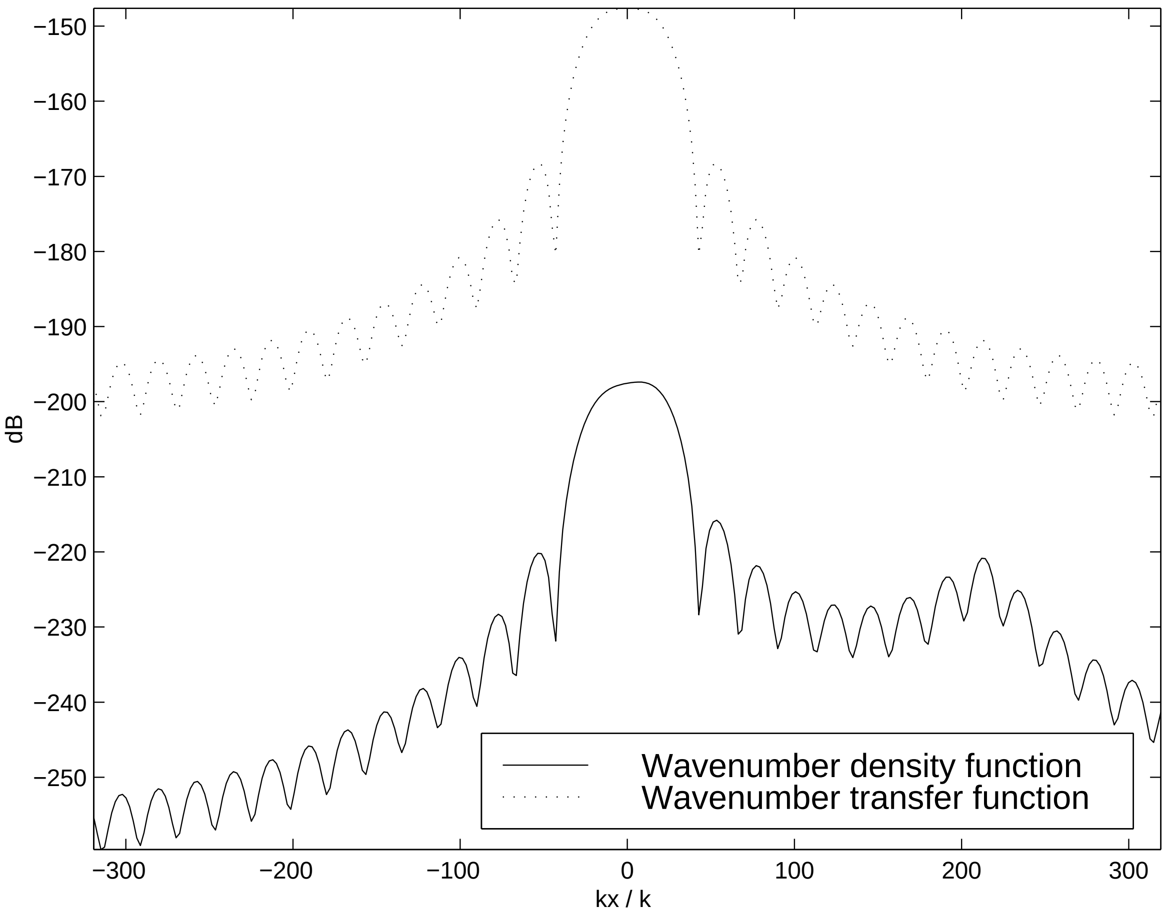

dB
−150
−160
−170
−180
−190
−200
−210
−220
−230
−240
−250
−300
−200
−100
0
100
200
300
kx / k
Wavenumber density function
Wavenumber transfer function

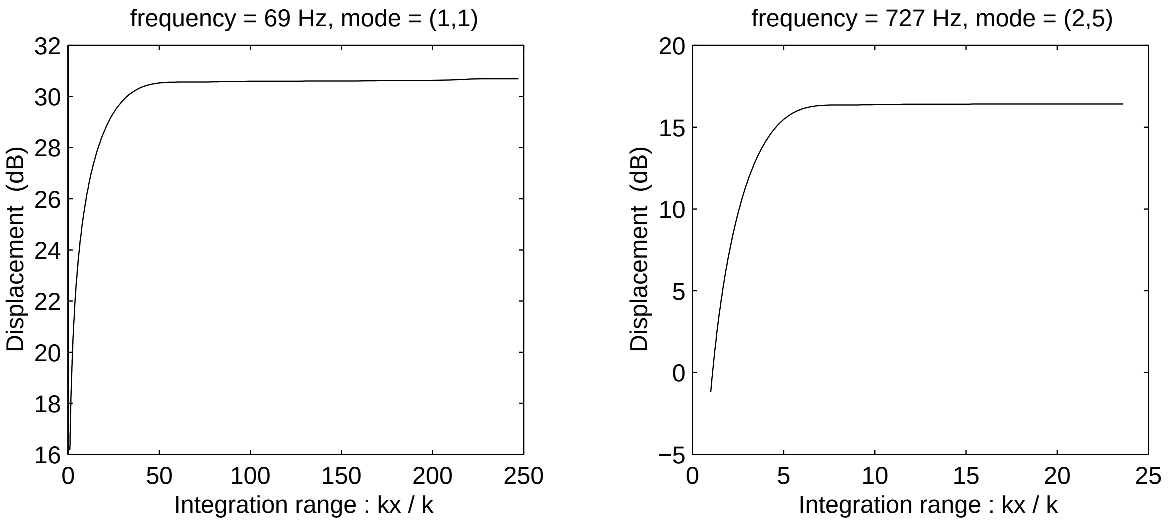
frequency = 69 Hz, mode = (1,1)
Displacement (dB)
Integration range : kx / k
frequency = 727 Hz, mode = (2,5)
Displacement (dB)
Integration range : kx / k

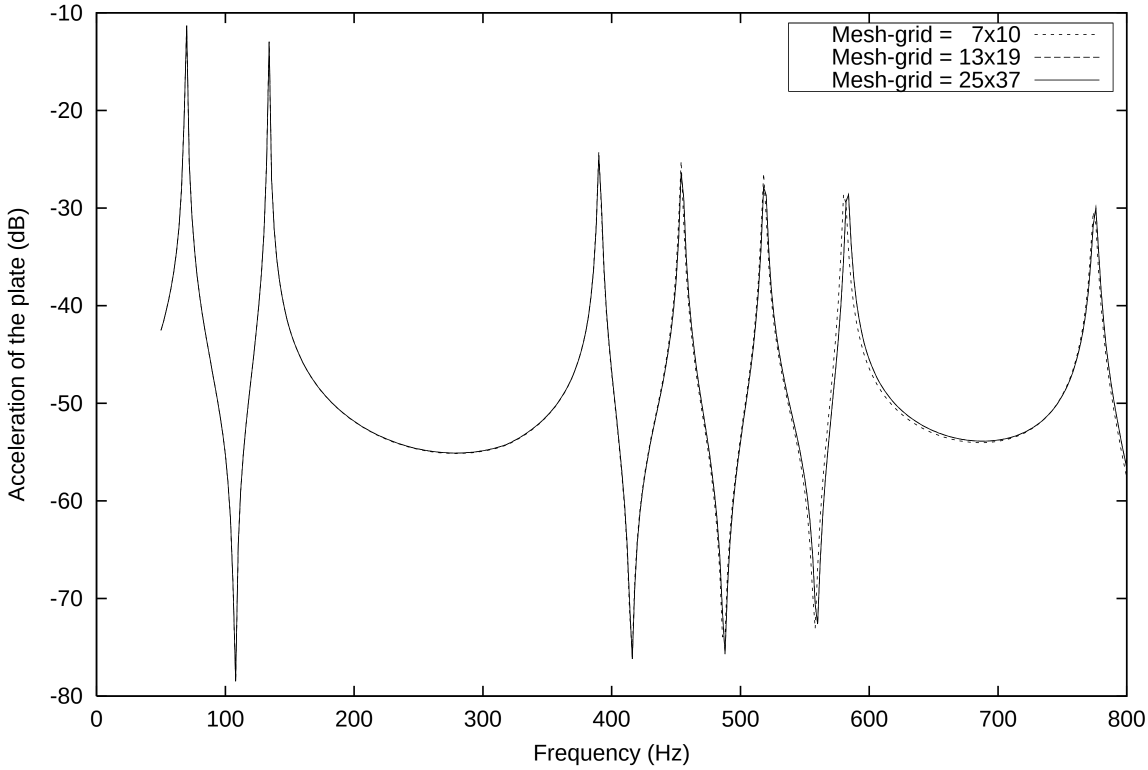

Mesh-grid = 7x10
Mesh-grid = 13x19
Mesh-grid = 25x37
Acceleration of the plate (dB)
Frequency (Hz)
-10
-20
-30
-40
-50
-60
-70
-80
0
100
200
300
400
500
600
700
800

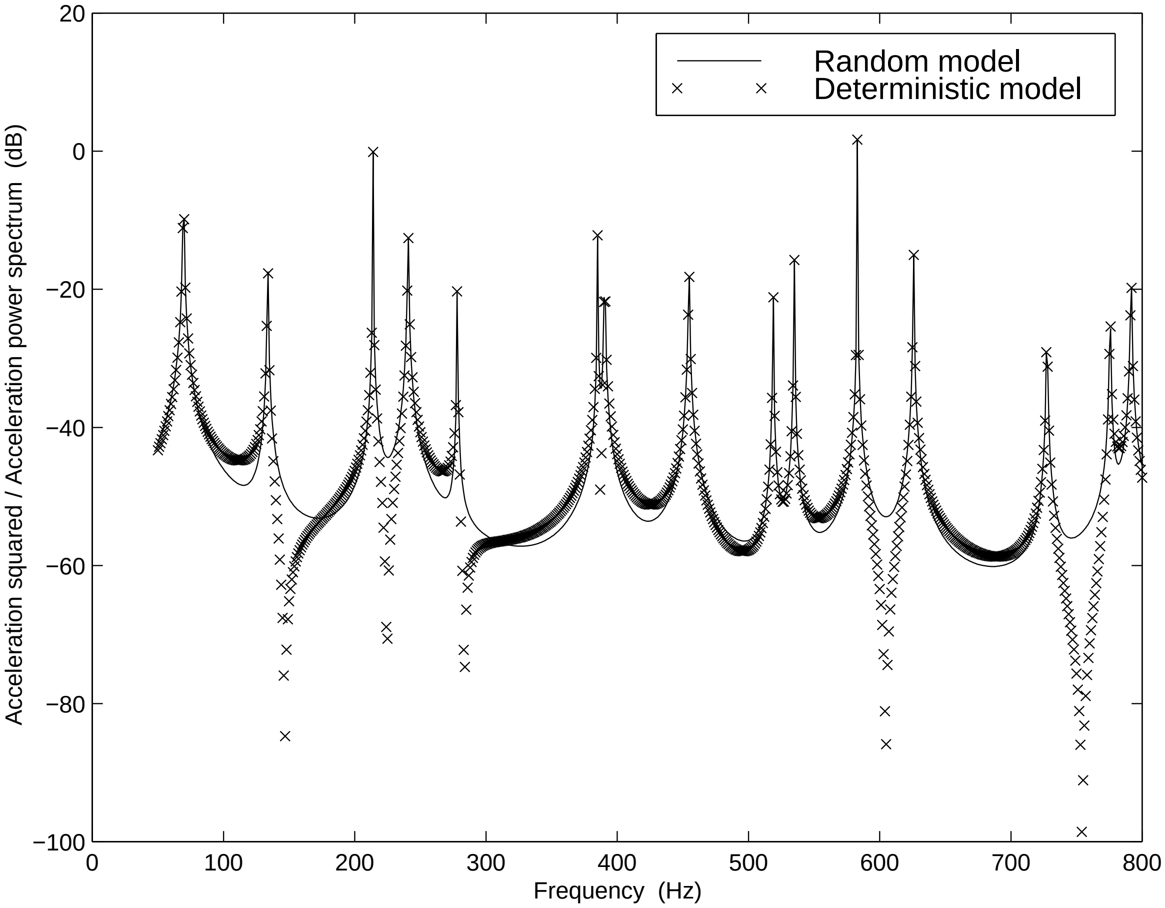
Random model
Deterministic model
Acceleration squared / Acceleration power spectrum (dB)
Frequency (Hz)
20
0
−20
−40
−60
−80
−100
0
100
200
300
400
500
600
700
800

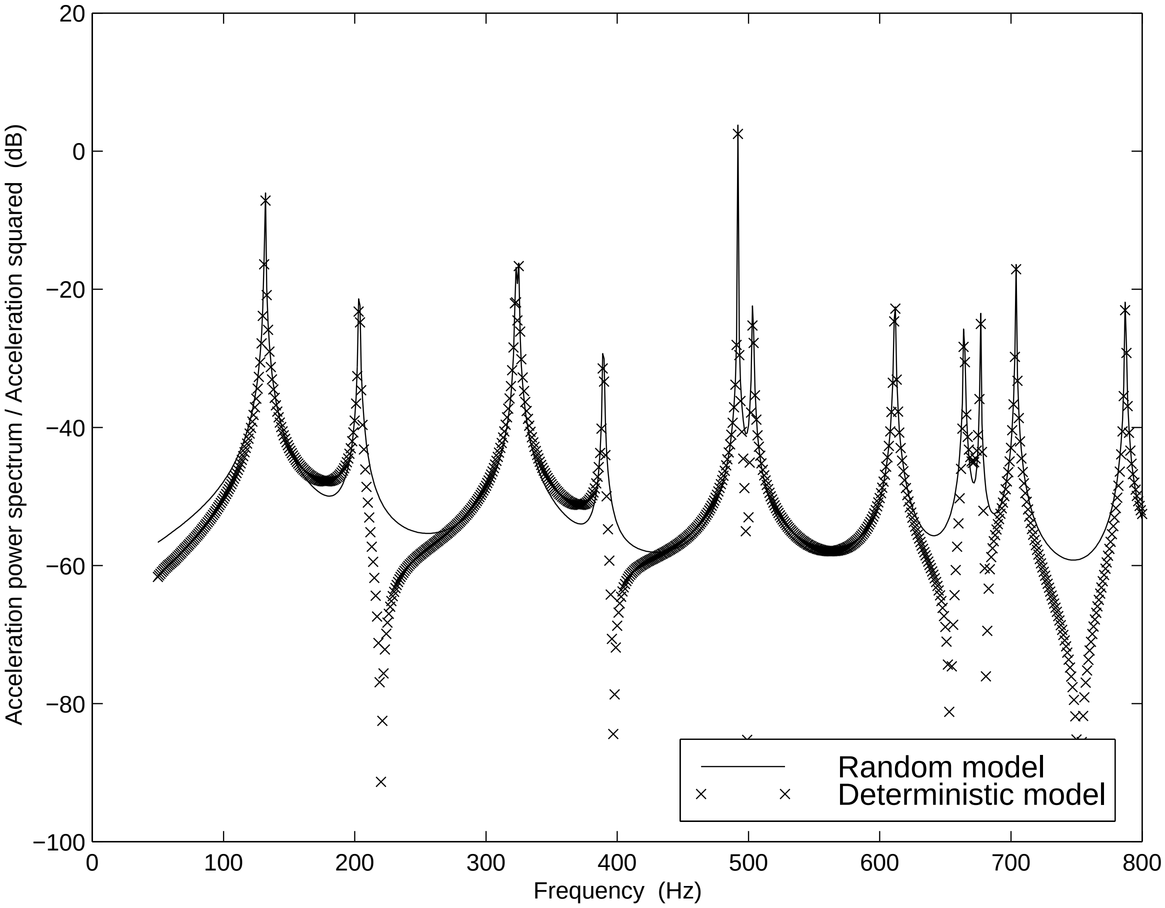

20
0
−20
−40
−60
−80
−100
0
100
200
300
400
500
600
700
800
Acceleration power spectrum / Acceleration squared (dB)
Frequency (Hz)
Random model
Deterministic model

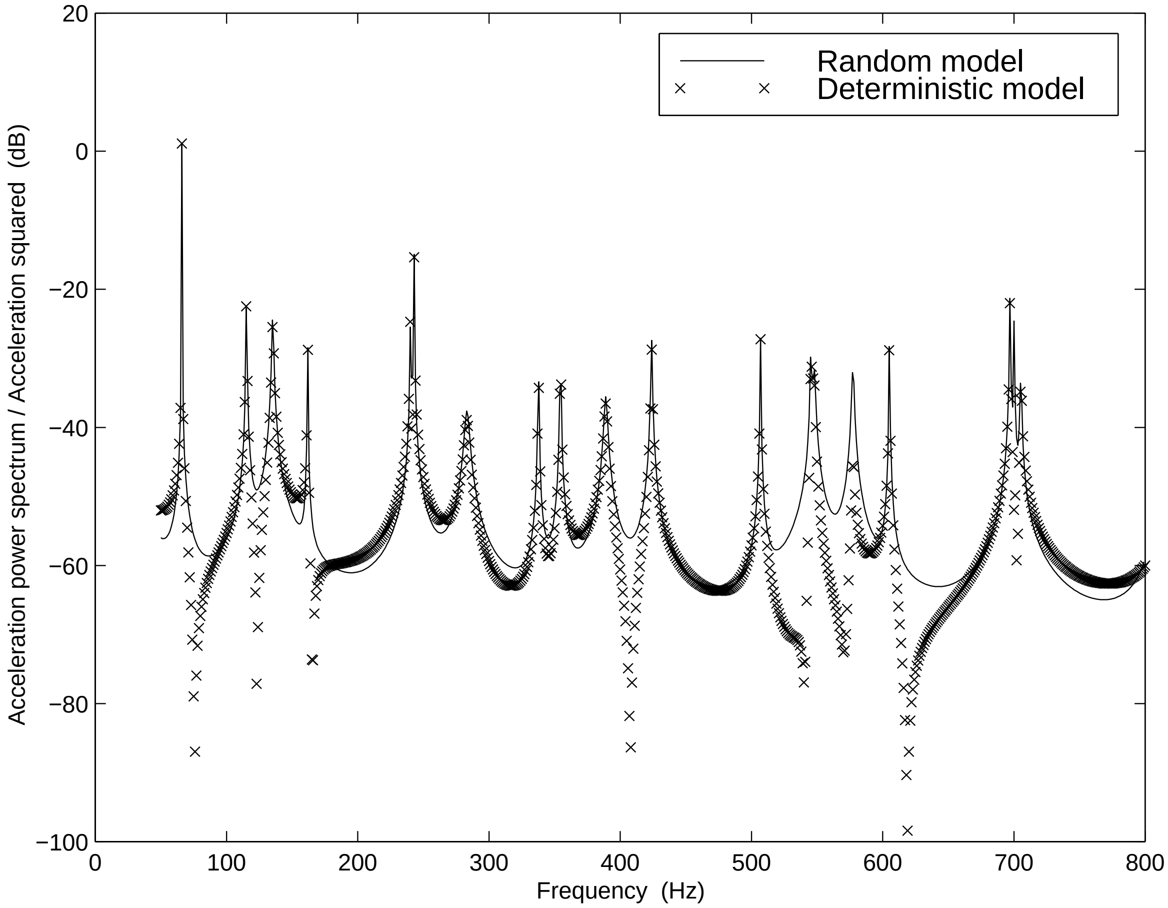

20
0
−20
−40
−60
−80
−100
0
100
200
300
400
500
600
700
800
Frequency (Hz)
Acceleration power spectrum / Acceleration squared (dB)
Random model
Deterministic model

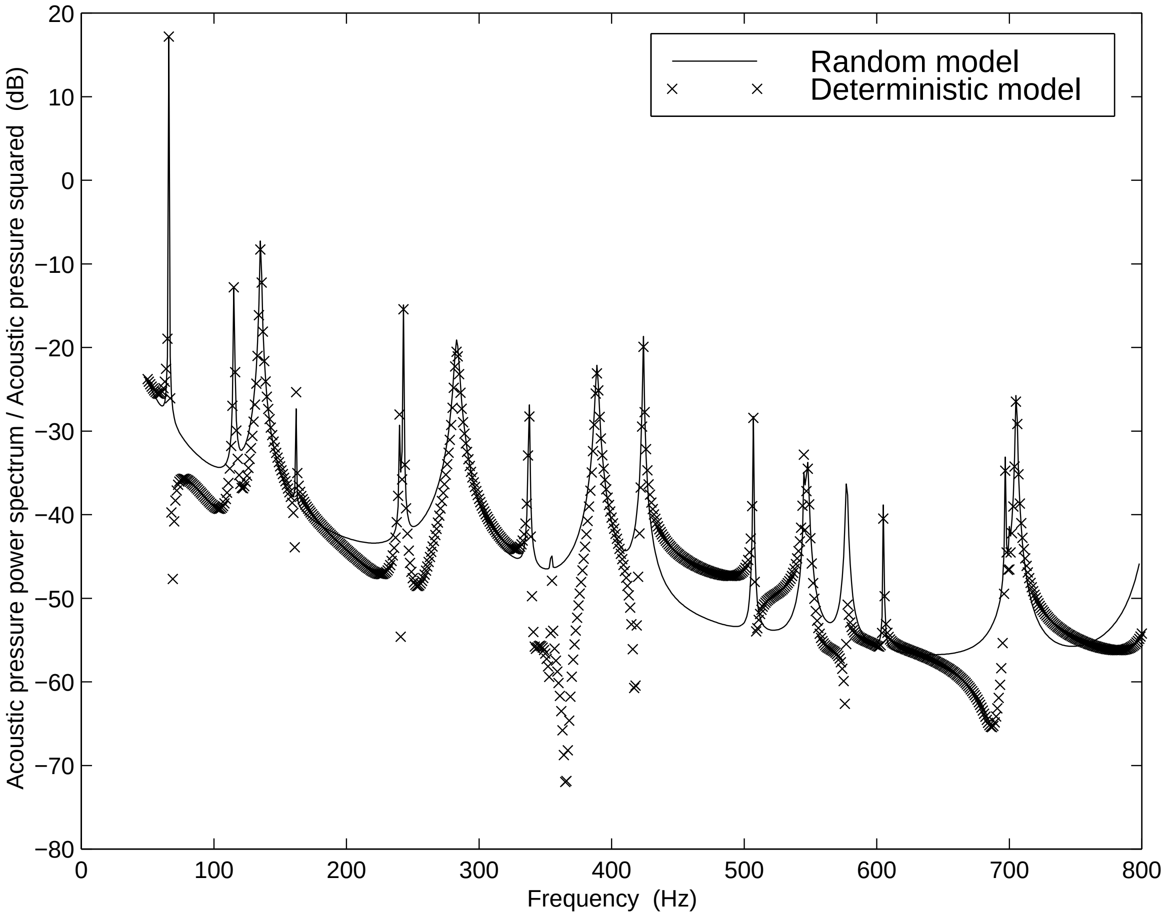
Random model
Deterministic model
Acoustic pressure power spectrum / Acoustic pressure squared (dB)
Frequency (Hz)
20
10
0
−10
−20
−30
−40
−50
−60
−70
−80
0
100
200
300
400
500
600
700
800

Figure 1 : Geometry of the structure.

Figure 2 : Corcos power spectrum in the plane $ky = 0$.

Figure 3 : Wavevector density and transfer functions of the displacement in the middle of the plate in the plane $ky = 0$.

Figure 4 : Influence of the wavenumber integration domain on the displacement.

Figure 5 : Mesh-grid refinement study.

Figure 6 : Acceleration of the simply supported plate *in vacuo* at point (0.33 m, 0.46 m).

Figure 7 : Acceleration of the clamped plate *in vacuo* at point (0.33 m, 0.46 m).

Figure 8 : Acceleration of the simply supported fluid-loaded plate at point (0.33 m, 0.46 m).

Figure 9 : Acoustic radiation of the simply supported fluid-loaded plate at point (0.33 m, 0.46 m, 0.5 m).